An FCC Compliant Pulse Generator for IR-UWB Communications

S. Bagga, S. A. P. Haddad, W. A. Serdijn and J. R. Long

***Abstract*—In [1], we have shown that it is feasible to design filters with arbitrary waveform responses and therefore we propose an ultra-wideband pulse generator incorporating a filter with a Daubechies' impulse response (i.e. maximally flat over the desired frequency range). This pulse generator is co-designed with wideband antennas. An eight-order Padé approximation of its transfer function is selected to implement the FCC stipulated frequency spectrum. Subsequently, the orthonormal [2] form is adopted, which is intrinsically semi-optimized for dynamic range, has low sensitivity to component mismatch, high sparsity and whose coefficients can be physically implemented. Each coefficient in the state-space description of the orthonormal ladder filter is implemented at circuit level using a novel 2-stage gm cell employing negative feedback. Simulation results in IBM's CMOS 0.13μm technology show that this pulse generator requires a total current of 25mA from a 1.2V power supply. The frequency coverage of the simulated waveform is about 85% of the FCC mask.**

***Index Terms*–analog integrated circuits, Daubechies' wavelets, filter approximation, low power, state-space description, impulse radio, ultra-wideband**

I. Introduction

Ultrawideband (UWB) technology has gained much interest during the last few years as a potential candidate for future wireless short-range data communication. A particular type of UWB communication is impulse radio, where very short transient pulses are transmitted rather than a modulated carrier. The United States Federal Communications Commission (FCC) has officially endorsed ultra-wideband technology for commercial wireless applications. Although impulse radio ultra-wideband technology promises enhanced data throughput with low-power consumption, it inseparably introduces several challenging design issues. The FCC allocated spectrum for UWB lies from 3.1-10.6GHz. As ultra-wideband systems transmit at very low spectral densities and occupy a large amount of bandwidth, it thus is unequivocal that the pulse generator's performance be optimized for maximum energy efficiency.

In literature, it is seen that one of the most attractive qualities of Daubechies' wavelets [3] is that they are window-like functions in the frequency domain. This single characteristic accounts for their unique localization property and therefore the Daubechies' wavelet can be used as the transmitted waveform in impulse radio UWB.

In Figures 1a and 1b show the mother wavelet and the scaling function of order 8, where the latter is often used to generate the mother wavelet.

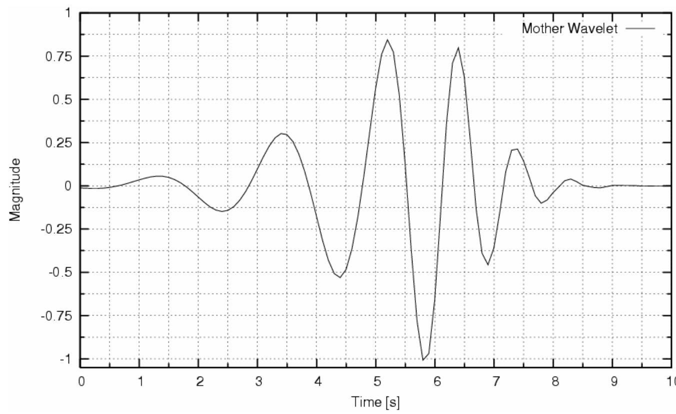

a) Mother Wavelet

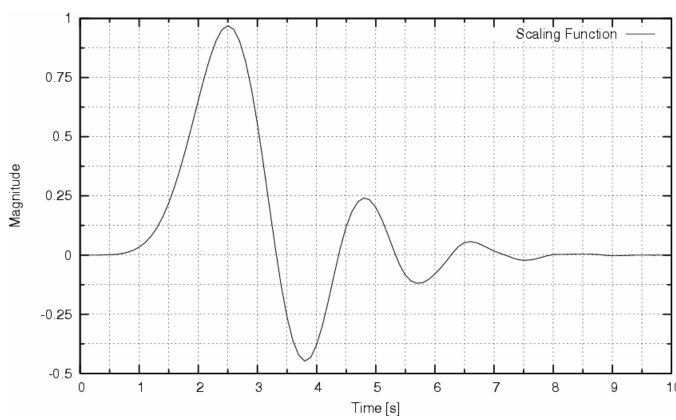

b) Scaling Function

Fig. 1 Daubechies' *Scaling and Mother Wavelets*

Like in [1], a transfer function whose impulse response approximates either the scaling or the mother wavelet can be generated. As Daubechies' wavelet functions are designed to have large number of zero crossings, for the simplification in numerical computation, the scaling function is chosen, which has fewer zero crossings. This property facilitates the transfer function design synthesis.

In this paper we propose an FCC compliant pulse generator for impulse radio ultrawideband communications. A system model is

S. Bagga, S. A. P. Haddad, Wouter A. Serdijn and John R. Long are with the Electronics Research Laboratory, Faculty of Electrical Engineering, Mathematics and Computer Science, Delft University of Technology, Mekelweg 4, 2628CD, Delft, The Netherlands (e-mail: {s.bagga, s.haddad, w.a.serdijn, j.r.long}@ewi.tudelft.nl).

shown in Section 2. Section 3 discusses the transformation procedure of the transfer function of the Daubechies' filter into the orthonormal state-space form. Transconductance amplifiers are frequently employed in filters designed for high-frequency applications and are thus also in this particular case of impulse radio ultra-wideband circuit design. Section 4 shows simulation data of the transconductance amplifier as well as the performance of the pulse generator. Section 5 presents the conclusions.

II. SYSTEM DESIGN

A. Pulse generator model

As seen in Fig. 2, by generating a window-like response in the baseband (i.e. with the Daubechies' filter) and then through upconversion, the energy spectrum of the pulse generator can be matched to that of the FCC frequency mask. The focus of this work is to implement the Daubechies' filter in CMOS technology. For detection in the receiver, the absolute shape of the transmitted waveform is not relevant as seen in [4]. Biphase modulation of the transmitted waveform can be achieved by alternating the polarities of the "impulses" that are used to drive the Daubechies' scaling function filter. In the next section, the transfer function of the Daubechies' filter is derived.

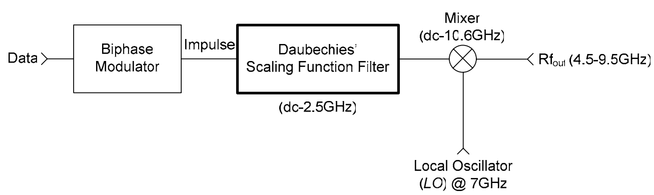

Fig. 2 Proposed pulse generator block diagram

B. Transfer function and state-space synthesis

Trade-offs between roll-off, attenuation and circuit complexity are taken into consideration prior to choosing the filter order of the Daubechies' filter. An eighth order filter is chosen with a bandwidth from dc-2.5GHz. The transfer function (as seen below) of the filter is generated using a Padé approximation [1]. The magnitude transfer as well as the phase response corresponds to that of a Daubechies' scaling function.

$$H(s)=\left[\frac{-33.9363s^5+2729.84s^4-67677.4s^3+959133s^2+4.38733e7s+2.94871e8}{s^8+62.9409s^7+2419.79s^6+63508s^5+1.19569e6s^4+1.617e7s^3+1.48766e8s^2+8.25321e8s+2.06313e9}\right]$$

Once the desired transfer function is formulated, its state-space description is then determined. A state-space description for a given transfer function is not unique, meaning that many state-space descriptions can implement the same transfer function. Moreover, a state-space description of any filter transfer function should be optimized for dynamic range, sensitivity, sparsity and coefficient values [1], [5].

C. Orthononormal ladder structure

Among known standard state-space descriptions, such as the canonical, the diagonal and the modal, the orthonormal ladder form is notable since it is by definition semi-optimized for dynamic range due to the specific structure of the matrices. Furthermore, since it is derived from a ladder structure, it is intrinsically less sensitive and the matrices are highly sparse.

A low sensitivity suppresses the effect of component variations on the transfer function. It can be proved that a filter that is optimized for dynamic range is also optimized for sensitivity [6]. A detailed explanation of the procedure to derive the orthonormal ladder form can be found in [2]. The sparsity of the matrices directly determines the circuit complexity. State-space descriptions of filters with more zero elements require less hardware and are likely to consume lower power. Thus, it is therefore an important design aspect of state-space filters. In respect to a fully optimized and fully dense state-space description [5], the resulting semi-optimal orthonormal filter structure differs only by about 2 dB in dynamic range. The A, B, and C matrices of the defined transfer function can be calculated as in [1].

D. Scaling –capacitance and coefficient values

Transconductance amplifiers will form the basic building blocks to implement the state-space description coefficients of the filer. The integrators are implemented as capacitors with a normalized value of 1F. The corresponding matrices *A*, *B*, and *C* have extremely large coefficients [1] corresponding to large gm values, which are not physically feasible at circuit level. By scaling down the capacitors (*cap*=0.1pF) and α_1, one consequently scales matrices *A* and *B*. Coefficients of matrix *C* can too be down scaled by α_2, without affecting the response of the filter.

$$\begin{aligned} A^* &= cap\cdot A \\ B^* &= \alpha_1\cdot cap\cdot B \\ C^* &= \alpha_2\cdot C \end{aligned} \qquad (1)$$

The block diagram of the state-space filter is shown in Fig. 3 and has 22 non-zero coefficients.

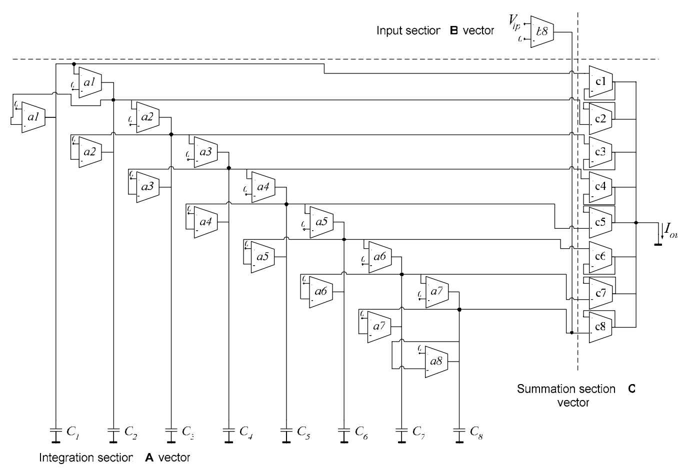

Fig. 3 Complete state-space filter structure

Once the block diagram has been recognized, a transconductance amplifier implements every coefficient.

III. TRANSCONDUCTANCE AMPLIFIER

The transconductance amplifier is implemented using a negative feedback structure consisting of an active circuit, which implements a nullor, and a feedback network (see Fig 4a).

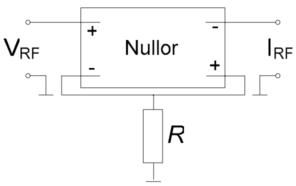

a) Negative feedback amplifier - *nullor*

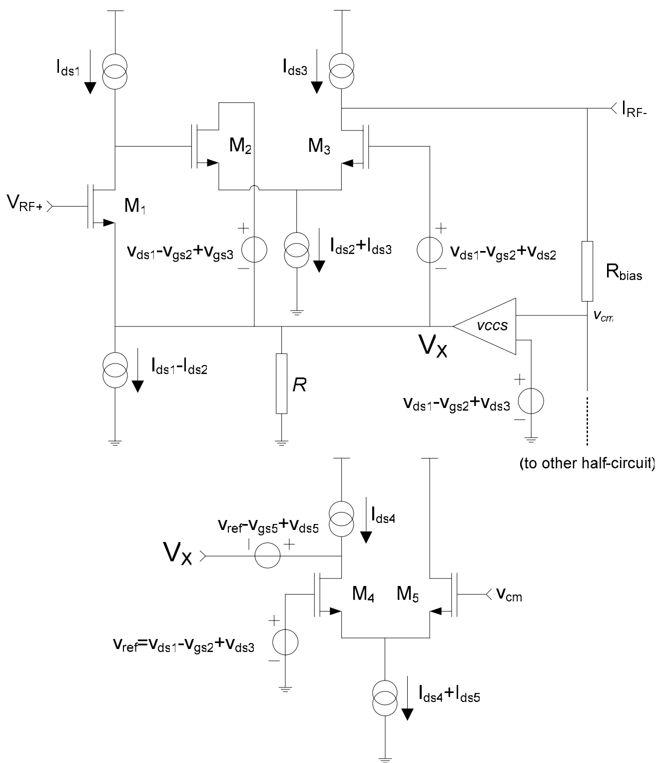

b) 2-stage implementation

Fig. 4 Negative feedback gm amplifier (half-circuit)

The orthonormal structure has both positive as well as negative coefficients. To implement a negative coefficient, a differential topology is used. Another advantage of using the latter is the cancellation of even order distortion terms that may arise from the actual nullor implementation, thus improving linearity.

The nullor (half circuit) is realized using a common source (*CS*) stage formed by transistor (M_1) at the input, and a non-inverting differential pair (M_2-M_3) at the output. The feedback network is made up of a resistor ***R*** (see Fig 4b).

As compared to a single-stage implementation, a 2-stage nullor improves the loop gain, which yields higher linearity as well as bandwidth [7] at the expense of power consumption. In reference to stability, frequency compensation in the form of pole-zero cancellation may be applied to this transconductance amplifier by means of a resistor-capacitor network connected between the gate of M_2 and the source of M_1. For biasing of the differential structure, the common-mode voltage (v_{cm}) is sensed at the outputs by R_{bias} and is compared to the desired reference voltage using a voltage-controlled current source (*VCCS*). Its implementation is shown on the left hand side of Fig. 4. The output current delivered by the VCCS is then applied to a virtual ground node, V_X.

IV. SIMULATION RESULTS

Fig. 5 shows the magnitude and phase response of the stand-alone transconductance amplifier used in this filter. The magnitude and the phase demonstrate a relatively flat response up to about 3GHz.

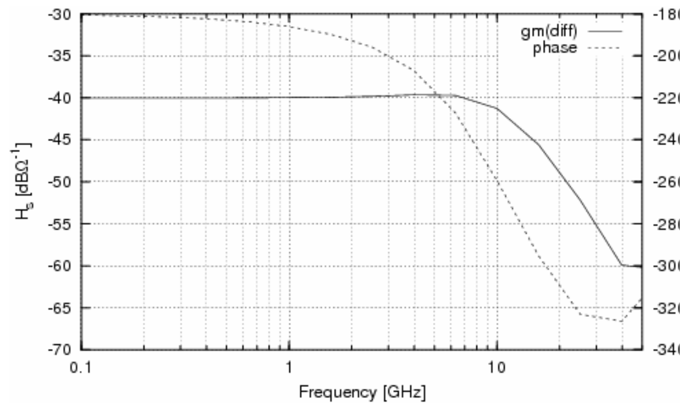

Fig. 5 Magnitude and phase transfer of stand-alone gm cell

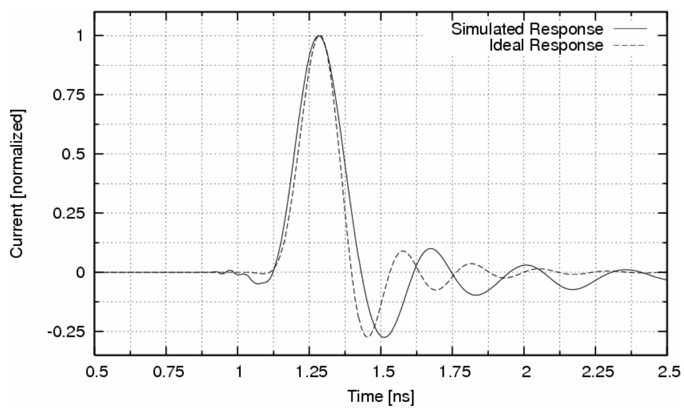

Fig. 6 Impulse response of an 8th order Daubechies' scaling function filter

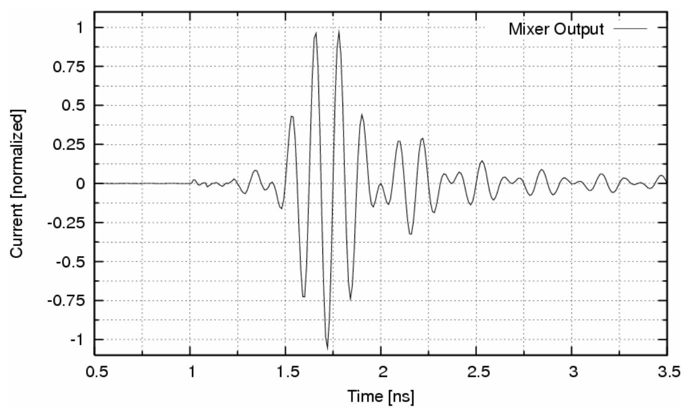

Fig. 7 Impulse response of an 8th order Daubechies' scaling function filter

The simulated impulse response of the Daubechies' scaling function filter and the upconverted waveform are seen in Fig. 6 and Fig. 7. By scaling down the capacitance even lower than 0.1pF as well as the coefficients in the matrices *A* and *B*, smaller pulse widths are attainable because of the trade-off between bandwidth and gain. Fig. 8 shows the frequency spectrum of the Daubechies' scaling function upconverted with a 7GHz carrier. As seen in the figure, the pulse generator's performance can now be optimized for maximum energy efficiency.

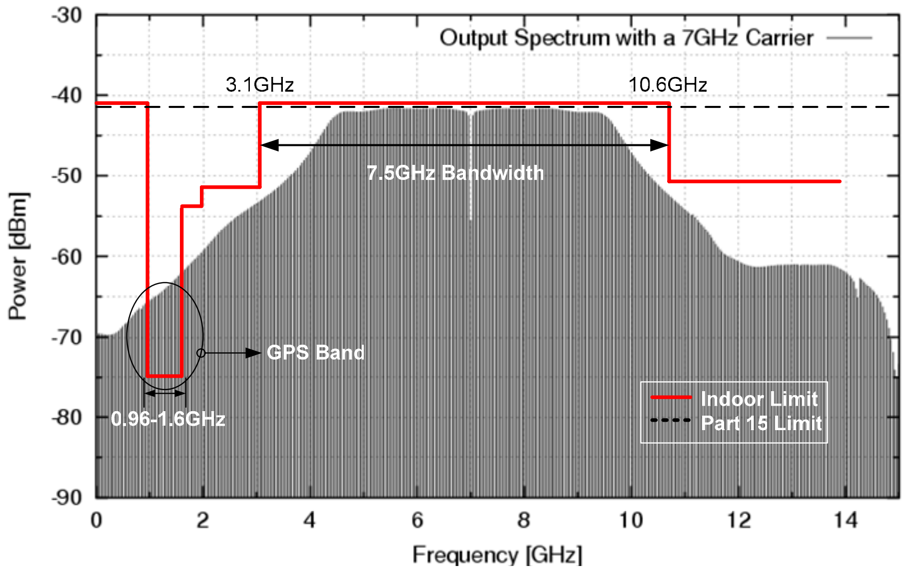

Fig. 8 Frequency spectrum of the upconverted waveform

It must be noted that there is still some residual signal in the 0.96-1.6GHz frequency band. However, this will be filtered out by the UWB antenna [8]. The simulation parameters of the delay filter are given in Table I.

TABLE I SIMULATION PARAMETERS

Specifications	Simulated
Waveform	Scaling Function of Daubechies' Mother Wavelet
Bandwidth	4.2-9.7GHz
Frequency coverage	@ 85%
Current consumption	25mA @ 1.2V
Size	1.25mm^2
Process	IBM CMOS 0.13µm

Finally, in line with [9] and [10] a Monte Carlo analysis reveals that the pulse shape is relatively unlikely to show discrepancy as a result of neither process variations nor component mismatches.

V. CONCLUSIONS

An FCC compliant pulse generator has been presented. An eighth order Padé approximation of the Daubechies' scaling function is selected. Subsequently, an orthonormal state-space approach is adopted, which fulfills the requirements of dynamic range, sensitivity, and sparsity. The coefficients are down scaled in conjunction with capacitance values. Each element of the filter is implemented at circuit level using a negative feedback 2-stage gm amplifier. After upconverting the scaling function, there is an 85% coverage of the FCC frequency spectrum for UWB applications. Simulation results in IBM's CMOS 0.13µm technology show that the Daubechies filter requires a total current of 25mA from a 1.2V power supply.

VI. REFERENCES

[1] S.A.P. Haddad, S. Bagga and W.A. Serdijn, "Log-Domain Wavelet Bases," in *Proceedings IEEE International Symposium of Circuits and Systems*, vol. 1, pp. 1100-1103, May 2004

[2] D.A. Johns, W.M. Snelgrove and A.S. Sedra, "Orthonormal Ladder Filters," *IEEE Transactions on Circuits and Systems*, vol. 36, pp. 337-343, March 1989

[3] I. Daubechies's, "Ten Lectures on Wavelets," *Society for Industrial and Applied Mathematics*, vol. 61, pp. 194-202, 1994

[4] Simon Lee, S. Bagga and W.A. Serdijn, "A Quadrature Downconversion Autocorrelation Receiver Architecture for UWB," *Joint UWBST and IWUWBS*, pp. 6-10, May 2004

[5] D. Rocha, "Optimal Design of Analogue Low-Power Systems: A strongly directional hearing-aid adapter," *PhD Thesis*, Delft University of Technology, 2003

[6] G. Groenewold, "*Optimal dynamic range integrators*", *IEEE Transactions on Circuits and Systems*, vol. 39, pp. 614-627, August 1992

[7] C.J.M.Verhoeven, A. van Staveren, G.L.E. Monna M.H.L. Kouwenhoven and E. Yildiz, "Structured Electronic Design: Negative-Feedback Amplifiers", Kluwer Academic Publishers, 2003

[8] S. Bagga, A. V. Vorobyov, S. A. P. Haddad, A. G. Yarovoy, W. A. Serdijn and J. R. Long, "Co-design of an Impulse Generator and Miniaturized Antennas for IR-UWB," in *Special Issue on UWB of the IEEE Transactions on MTT*, April 2006

[9] S. Bagga, S. A. P. Haddad, W. A. Serdijn, J.R. Long and E.B. Busking, "A Delay Filter for an IR-UWB Front-End," *IEEE International Conference on Ultra-Wideband*, pp. 323-327, September 2005

[10] S. Bagga, S. A. P. Haddad, K. van Hartingsveldt, S Lee, W. A. Serdijn and J.R. Long, "An interference rejection filter for an ultra-wideband quadrature downconversion autocorrelation receiver," *IEEE International Symposium on Circuits and Systems*, vol. 6, pp. 5357-5360, May 2005